A "moving metal mechanism" for substrate cleavage by the DNA repair endonuclease APE-1

ARTICLE *in* PROTEINS STRUCTURE FUNCTION AND BIOINFORMATICS · JULY 2007

Impact Factor: 2.63 · DOI: 10.1002/prot.21397 · Source: PubMed

6 AUTHORS, INCLUDING:

Numan Oezguen
Baylor College of Medicine
36 PUBLICATIONS **899** CITATIONS
SEE PROFILE

Catherine H Schein
Foundation for Applied Molecular Evolution
118 PUBLICATIONS **2,784** CITATIONS
SEE PROFILE

Werner Braun
University of Texas Medical Branch at Galves…
145 PUBLICATIONS **11,195** CITATIONS
SEE PROFILE

PROTEINS: Structure, Function, and Bioinformatics 68:313–323 (2007)

A "Moving Metal Mechanism" for Substrate Cleavage by the DNA Repair Endonuclease APE-1

Numan Oezguen,[1,2] Catherine H. Schein,[1,2,3,4] Srinivasa R. Peddi,[5] Trevor D. Power,[1,2] Tadahide Izumi,[5] and Werner Braun[1,2]*

[1]*Department of Biochemistry and Molecular Biology, University of Texas Medical Branch, Galveston, Texas 77555-0857*
[2]*Sealy Center for Structural Biology and Molecular Biophysics, University of Texas Medical Branch, Galveston, Texas 77555-0857*
[3]*Department of Microbiology and Immunology, University of Texas Medical Branch, Galveston, Texas 77555-0857*
[4]*Sealy Center for Vaccine Development, University of Texas Medical Branch, Galveston, Texas 77555-0857*
[5]*Department of Otorhinolaryngology, Louisiana State University, New Orleans, Louisiana 70112*

ABSTRACT **Apurinic/apyrimidinic endonuclease (APE-1) is essential for base excision repair (BER) of damaged DNA. Here molecular dynamics (MD) simulations of APE1 complexed with cleaved and uncleaved damaged DNA were used to determine the role and position of the metal ion(s) in the active site before and after DNA cleavage. The simulations started from an energy minimized wild-type structure of the metal-free APE1/damaged-DNA complex (1DE8). A grid search with one Mg^{2+} ion located two low energy clusters of Mg^{2+} consistent with the experimentally determined metal ion positions. At the start of the longer MD simulations, Mg^{2+} ions were placed at different positions as seen in the crystal structures and the movement of the ion was followed over the course of the trajectory. Our analysis suggests a "moving metal mechanism" in which one Mg^{2+} ion moves from the B- (more buried) to the A-site during substrate cleavage. The anticipated inversion of the phosphate oxygens occurs during the in-line cleavage reaction. Experimental results, which show competition between Ca^{2+} and Mg^{2+} for catalyzing the reaction, and high concentrations of Mg^{2+} are inihibitory, indicate that both sites cannot be simultaneously occupied for maximal activity. Proteins 2007;68:313–323.** © 2007 Wiley-Liss, Inc.

Key words: molecular dynamic simulation; divalent metal ion; BER-pathway

INTRODUCTION

The DNA of living cells is constantly subjected to intrinsic and extrinsic damage caused by polymerase errors, ionizing radiation, and chemical agents.[1,2] Cellular survival thus depends on DNA-repair mechanisms. One pathway, conserved from bacteria to humans, is that of "base excision repair" (BER),[3–13] which repairs damaged bases and apurinic/apyriminidic (AP) sites, generated by spontaneous, chemically induced or enzyme-catalyzed hydrolysis of the N-glycosyl bond. The first step in the BER pathway is the recognition of the damaged base by DNA glycosylases and removal of the damaged base, to create an AP site. This site is then recognized by apurinic/apyrimidinic endonuclease (APE1 in humans). APE1, also known as Ref-1 and HAP1, hydrolyzes the phosphodiester backbone 5′ to the AP site to create a 3′-OH group that can be recognized by DNA polymerase. Thus the cleavage reaction of APE1 needs to be understood not just in how it cleaves its substrate, but also according to how well it functions in collaboration with other enzymes in the BER pathway.[14,15]

While metal ions (Mg^{2+} is preferred) are required for activity of APE1, their biochemical role in catalysis has not been resolved. Several high resolution crystal structures of APE1 alone or in complex with DNA have indicated positions for one- or two-metal ions in the active site depending on the pH conditions (Table I). Low pH structures, such as 1DE9[16] or 1HD7,[18] have one-metal ion near the active site (A-site), whereas the neutral pH structure 1E9N[18] has an additional Pb^{2+} ion at a more buried site (B-site). The crystal structures 1DE8,[16] 1DEW,[16] and 1DE9[16] have DNA bound to APE1. In 1DE9 the DNA is cleaved and a Mn^{2+} ion is present (A-site). Other work has shown that the type of metal ion and ligand present during the crystallization can alter number and position of the metal ions in the active site.[19–25] This makes it difficult to conclude the role of the metal ions during the reaction. A two-metal mechanism is widely accepted in the catalytic steps of related enzymes, such as restriction endonucleases[26–29] and phosphatases,[30–35] however, the two-metal ions in those enzymes are held in place by a bridging network of car-

The Supplementary Material referred to in this article can be found online at http://www.interscience.wiley.com/jpages/0887-3585/suppmat/

Grant sponsor: National Computational Science Alliance (NCSA); Grant number: MCB020004N; Grant sponsor: Department of Energy; Grant number: DE-FG02-04ER63826; Grant sponsor: NIH; Grant number: CA98664

*Correspondence to: Werner Braun, BMB-SCSB, University of Texas Medical Branch, 301 University Boulevard, Galveston, TX 77555-0857. E-mail: webraun@utmb.edu

Received 23 May 2006; Revised 11 December 2006; Accepted 22 December 2006

Published online 11 April 2007 in Wiley InterScience (www.interscience.wiley.com). DOI: 10.1002/prot.21397

TABLE I. Metal Ion and Substrates/Product in the Crystal Structures of APE1 Referred to in This Paper

PDB-code	Resolution	Metal ions	DNA
1DE8[a]	2.9 Å	—	Not cleaved with one AP site (11 bp)
1DEW[a]	2.7 Å	—	Not cleaved DNA with one AP site (15 bp)
1DE9[a]	3.0 Å	Mn^{2+}	Cleaved 5′ to the AP site (9 bp)
1BIX[b]	2.2 Å	4 Sm^{3+}, Pt^{2+} (one Sm^{3+} at the active site)	—
1HD7[c]	2.0 Å	Pb^{2+} (at the active site)	—
1E9N[c]	2.2 Å	2 Pb^{2+} (both at the active site)	—

[a]Ref. 16.
[b]Ref. 17.
[c]Ref. 18.

boxylates at a much shorter distance when compared with the distance between two Mg^{2+} ions at the A- and B-site, and can therefore not be used as an explanation for the APE1 catalysis.

In our previous work, we analyzed the sequence and structural motifs of APE1 ("molegos") that are involved in metal binding and specific recognition of damaged DNA.[36–38] Here, we address the question of how the Mg^{2+} cofactor(s) functions during cleavage of the DNA and particularly whether the second, "B-site," observed only in the presence of Pb^{2+} and without the substrate, might be physiologically relevant. To begin, we performed a grid search to determine the low energy positions for one-metal ion. We further ran molecular dynamics (MD)-simulations series with complexes of APE1 with either cleaved or uncleaved damaged DNA, starting with Mg^{2+} ion(s) at different positions. The movements observed in the active site, interpreted in light of mutagenesis data, indicate that there are indeed two distinct stable positions for metal ions in the active site of APE1, which agree approximately with the positions where metal ions have been observed in the crystal structures. We propose a novel mechanism for the catalytic reaction, in which the metal moves from the more buried B-site to the A-site, seen in most of the crystal structures.

METHODS

The coordinates of the crystal structure 1DE8[16] were used to generate a model of the wild-type APE1-DNA complex. The DNA had 11 base pairs with a noncleaved AP site. All buried crystal water molecules were treated as part of the complex and were included in the simulations. The starting positions of the Mg^{2+} ions were determined by superimposing the model with the crystal structures 1DE9[16] and 1E9N.[18] In the systematic search the ions were placed at grid points with 0.8 Å space between the points in each direction. The grid was defined by shifting the origin of the new coordinate system to the A-site, as defined by Beernink et al.[18] (1E9N). The new x-axis was defined as the direction from the A-site to the B-site, the second Pb^{2+} position in 1E9N. Finally the y- and z-axes were constructed perpendicular to the new x-axis. The range of the grid was in x-direction [−3.2 Å, 8.0 Å] and [−3.2 Å, 3.2 Å] in y- and z-directions with 1215 grid points.

Na^+ ions were added to the complexes of APE1-DNA-Mg^{2+} to achieve electrostatic neutrality. The counter ions were positioned on appropriate points on a 1 Å grid, which was overlaid on the system. In the next step the whole system of crystal water molecules, counter ions, APE1, cleaved or uncleaved DNA, and Mg^{2+} ion(s) were soaked in TIP3 water box.[39] The borders of the water box were extended at least 7 Å beyond any system atom. The final box dimensions were typically $71 \times 71 \times 77$ Å^3 with 8626 water molecules and the APE1-DNA-Mg^{2+}-Na^+ complex. Counter ions and the water box were added using the XLEAP module of the AMBER 6.0 distribution.

The AMBER force field does not have parameters for nonstandard residues such as the uncleaved or cleaved AP site. The parameters for the uncleaved AP site were obtained from Roman Osman's group at Mount Sinai School of Medicine, Physiology and Biophysics Department, New York. The parameters for the cleaved AP site were generated in house, in the same way as Roman Osman's group, following the procedure described in the AMBER manual for determining parameter for new compounds. Herein the RESP charge fitting algorithm, a utility distributed with the AMBER 6.0, was used. The input for RESP was generated in a three-cycle procedure utilizing the Merz–Singh–Kollman[40,41] electrostatic potential charge fitting analysis from an ab initio gas-phase calculation in GAUSSIAN98[42] at the Hartree–Fock level in basis set 6-31G(d).

For all simulations the system was energy minimized over 2000 steps with periodic boundary conditions using standard protocol to relax steric clashes. Molecular dynamic simulation over 500 or 20 ps in the case of the systematic grid search followed. The parameters of the MD simulations were periodic boundary conditions, Particle Mesh Ewald summation of the nonbonded interactions, constant temperature (300 K), constant pressure (1 bar), 1 fs per step, and parm99 force field.[43] All minimizations and MD simulations were performed using the SANDER module.

The analysis was done with MOLMOL,[44] the modules ANAL and CARNAL from the AMBER 6.0 distribution, and PERL scripts. MOLMOL was also used to generate the figures. With ANAL the potential energies of the Mg^{2+} ions were determined using a 15 Å cutoff.

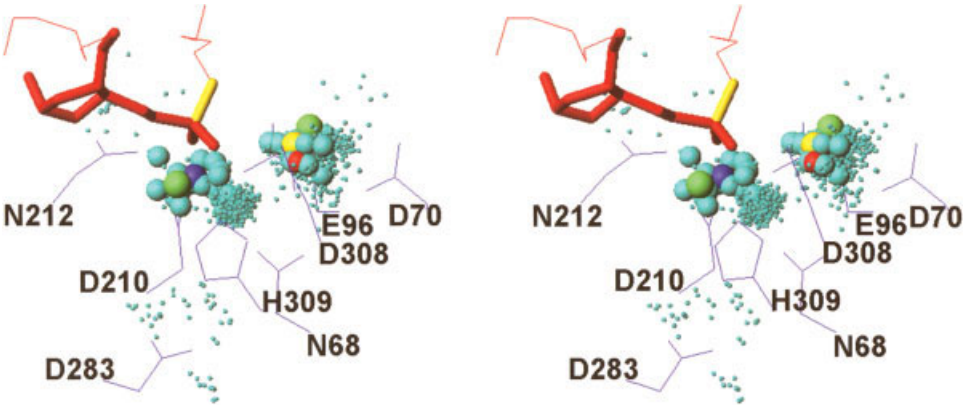

Fig. 1. Positions of Mg^{2+} ions after initial minimization, followed by a 20 ps MD simulation at 300 K, and final minimization. The Mg^{2+} ions were positioned in the beginning on 0.8 Å spaced 1215 points grid (one ion per simulation). The AP-site is shown in thicker red lines. Important side chains are shown in blue. The Mg^{2+} final positions are shown in cyan. The 50 positions with lowest potential energy are shown in larger spheres. The position of the lowest energy is colored in blue and the third lowest energy position is colored in red. They correspond to the B- and A-site. The two Pb^{2+} from 1E9N and the Mn^{2+} from 1DE9 are shown in green and yellow. The bond to be cleaved is shown also in yellow.

RESULTS

Determining Low Energy Positions for Mg^{2+} in the Active Site

To determine the most likely position(s) for metal ions in the active site, a systematic search for local potential energy minima for one Mg^{2+} ion was done. A complex, comprised of an 11 base pair DNA with an uncleaved AP site bound to one molecule of APE1, one Mg^{2+} ion, and 16 Na^{+} counter ions, was soaked in a TIP3 water box. The metal ion was placed on grid positions in the active site region, determined as described in Methods. The active site histidine, H309, was protonated, to be consistent with its suggested role in catalysis, in which it forms a hydrogen bond to the O1P of the AP phosphate.[11,16,18] A point mutation, H309N, abolishes endonuclease activity and increases the rate of substrate release 10 fold compared with WT APE1.[45,46]

The system was initially minimized, followed by a 20 ps MD simulation at 300 K. Finally it was minimized again before analyzing the potential energy of the Mg^{2+} ion by summing all nonbonded interaction energies with atoms within 15 Å.

Of the initial 1215 Mg^{2+} positions tested, 67 crashed due to steric clashes with another atom in the complex, which caused very high gradient/force (repulsive van der Waals contributions). The final positions of the Mg^{2+} ions in the remaining 1148 runs clustered at positions consistent with crystal structures (see Fig. 1). The two lowest potential energy positions (−292.2 and −283.1 kcal/mol) were closest to the "B-site," that is, the site of the second, more buried Pb^{2+} in the 1E9N crystal structure (Table II). The distance was 2.5 Å (Table III). The other ions centered around the third lowest energy position (−281.4 kcal/mol), our "grid A-site," which encompassed the experimentally determined positions for Sm^{3+} and Mn^{2+} in the crystal structures 1BIX and 1DE9 and that of the second Pb^{2+} ion in 1E9N, all of which lie 0.8–1.8 Å from the center of the cluster (Table III).

TABLE II. Ten Lowest Potential Energies (in kcal/mol) for One Mg^{2+} Ion in the Grid Search (Precleavage)

Run no.	E_{Tot}	$E_{Coulomb}$	E_{vdW}	Site
660	−292.2	−318.1	25.9	B
649	−283.1	−309.7	26.7	B
584	−281.4	−305.2	23.8	A
1080	−281.2	−308.5	27.3	A
440	−279.9	−302.0	22.1	A
979	−276.5	−303.8	27.3	B
1136	−274.8	−299.8	25.0	B
503	−274.0	−299.4	25.5	A
737	−273.5	−294.8	21.3	A
820	−273.3	−305.2	31.9	B

A- and B-Sites of APE1 are not Typical of Other "Two-Metal" Transphosphorylation Centers

While a two-metal mechanism has been suggested for APE1 cleavage of the DNA backbone at abasic sites, the stable grid positions are much further apart than those in phosphatases and polymerases.[38] The two-metal ion catalytic sites in phosphatases are within a short (<4.0 Å) distance of one another, with a bridging network of negatively charged protein side chains to mitigate their repulsive interactions.[38,47,48] In contrast, the two sites defined experimentally and by our grid search for APE1 (see Fig. 2) are 5.7 Å apart, and the two Pb^{2+} ions in the 1E9N crystal are 5.1 Å apart. These distances are similar to the intermetal distances in restriction endonucleases.[26,27] However, when two-metal ions are placed at both sites, by the end of the 500 ps simulations they move even further away from one another, to 7.6–7.7 Å (Fig. 3 and Table III). In the same simulations the

TABLE III. Distances (in Å) Between the Metal Ion Positions in the Crystal Structures and the Final Position of the Metal Ions in Our Grid Search and Simulations

		1BIX Sm^{3+}	1DE9 Mn^{2+}	1E9N Pb^{2+}		1HD7 Pb^{2+}	Grid Mg^{2+}		MD-(A+B)[a]		MD-(A+B)[b]		MD (B→A)[c]
		A	A	A	B	A	Third lowest A	Lowest B	A	B	A	B	A
1BIX Sm^{3+}	A	0.0	1.6	0.9	6.0	0.5	1.7	6.1	2.9	7.0	2.5	6.8	2.9
1DE9 Mn^{2+}	A	—	0.0	1.0	4.5	1.8	0.8	5.0	2.7	5.8	2.5	5.6	1.7
1E9N Pb^{2+}	A	—	—	0.0	5.1	1.2	1.5	5.2	3.1	6.1	2.9	5.9	2.4
	B	—	—	—	0.0	6.2	5.0	2.5	6.3	2.7	6.5	2.0	4.0
1HD7 Pb^{2+}	A	—	—	—	—	0.0	1.8	6.3	2.6	7.2	2.2	7.1	2.9
Grid Mg^{2+}	Third lowest A	—	—	—	—	—	0.0	5.7	2.4	6.5	2.0	6.2	2.0
	Lowest B	—	—	—	—	—	—	0.0	6.8	0.9	7.2	1.2	4.6
MD-(A+B)[a]	A	—	—	—	—	—	—	—	0.0	7.6	1.0	8.0	2.3
	B	—	—	—	—	—	—	—	—	0.0	7.5	0.9	5.4
MD-(A+B)[b]	A	—	—	—	—	—	—	—	—	—	0.0	7.7	2.7
	B	—	—	—	—	—	—	—	—	—	—	0.0	5.2

The calculated structures were overlaid with the crystal structures using the MOLMOL program to determine the differences in the metal ion positions.
[a]MD simulation with the two Mg^{2+} ions starting at the Pb^{2+} positions in 1E9N. The DNA was not cleaved but H309 was protonated.
[b]Continuation of the simulation, which was started with the two Mg^{2+} ions in 1E9N positions. The DNA was cleaved and H309 and D210 were protonated.
[c]MD simulation with cleaved DNA, protonated D210 and H309. The metal starting position was the B-site. It moved during the simulation to the A-site.

distance between site-A metal and the leaving group is 5.2 Å pre-cleavage and 3.9 Å after cleavage (Table IV). After cleavage the distance is shorter because the new 3′ end moves toward the metal ion. The metal ion is too far away to stabilize the leaving group as suggested in the literature.[18] Thus both metals cannot be simultaneously bound in the active site in catalytically relevant positions. This is consistent with the literature[18,49] and our experimental data (Table V), which show negative effects of Ca^{2+}, a noncatalytic metal, on Mg^{2+}-based substrate cleavage by APE1, and the decrease in activity of APE1 at high Mg^{2+} concentrations, where both sites might be expected to be filled.

MD Simulations Offer Evidence for Two Metal Positions, in the Presence of Uncleaved Substrate

Simulations with one-metal ion placed at one or the other site emphasize that the B-site, which is found experimentally in only one of the crystal structures, is actually the most stable position for the metal ion in the presence of an uncleaved substrate (Table II). In simulations with uncleaved substrate, Mg^{2+} placed at the B-site remained there or moved to the B-site if placed a small distance away. Also, Mg^{2+} ions placed exactly at the crystal positions of Mn^{2+} (1DE9), Sm^{3+} (1BIX), or Pb^{2+} (1E9N), closest to the "grid A-site," moved to the B-site within the minimization steps. However the Mg^{2+} remained stable over 500 ps when placed at the grid A-site.

The side chain of N212 in the active site of APE1 formed H-bonds to the AP site of the substrate, whether Mg^{2+} was placed at the A- or B-site (Fig. 2). In both cases, H309 formed a very stable H-bond chain from D283 and to the substrate AP site (O2P or O1P). The Mg^{2+} ion at the B-site was octahedrally coordinated by both oxygen atoms of D210 and ProR oxygen atom (O2P) of the phosphate, E96, and N212 and a water molecule [Fig. 2(b)]. The major difference between the A- and B-site was that the Mg^{2+} at the B-site was 1.9 Å away from O2P, while when it was at the A-site, it was on the other side of the DNA backbone of the AP site and octahedrally coordinated by O1P, D308, D70, a water molecule, and both oxygens of E96 [Fig. 2(a) and Table IV].

The Mg^{2+} Ion Starting at the B-Site Moves to the A-Site After Cleavage

While crystal structures are limited to providing information about the active site before and after cleavage, MD simulations can be used to follow the trajectories during the reaction. For this purpose, simulations were set up with the metal ion placed in the final grid B-site conformation. In three independent simulations where both D210 and H309 were protonated and the substrate was cleaved artificially, the metal migrated from the B- to the A-site, a total distance of 4.6 Å. It moved 1.8 Å during the initial minimization of the complex, and an additional 3.3 Å after about 280 ps of simulation (Fig. 4). The 5′ (phosphate) position was unchanged, while the new

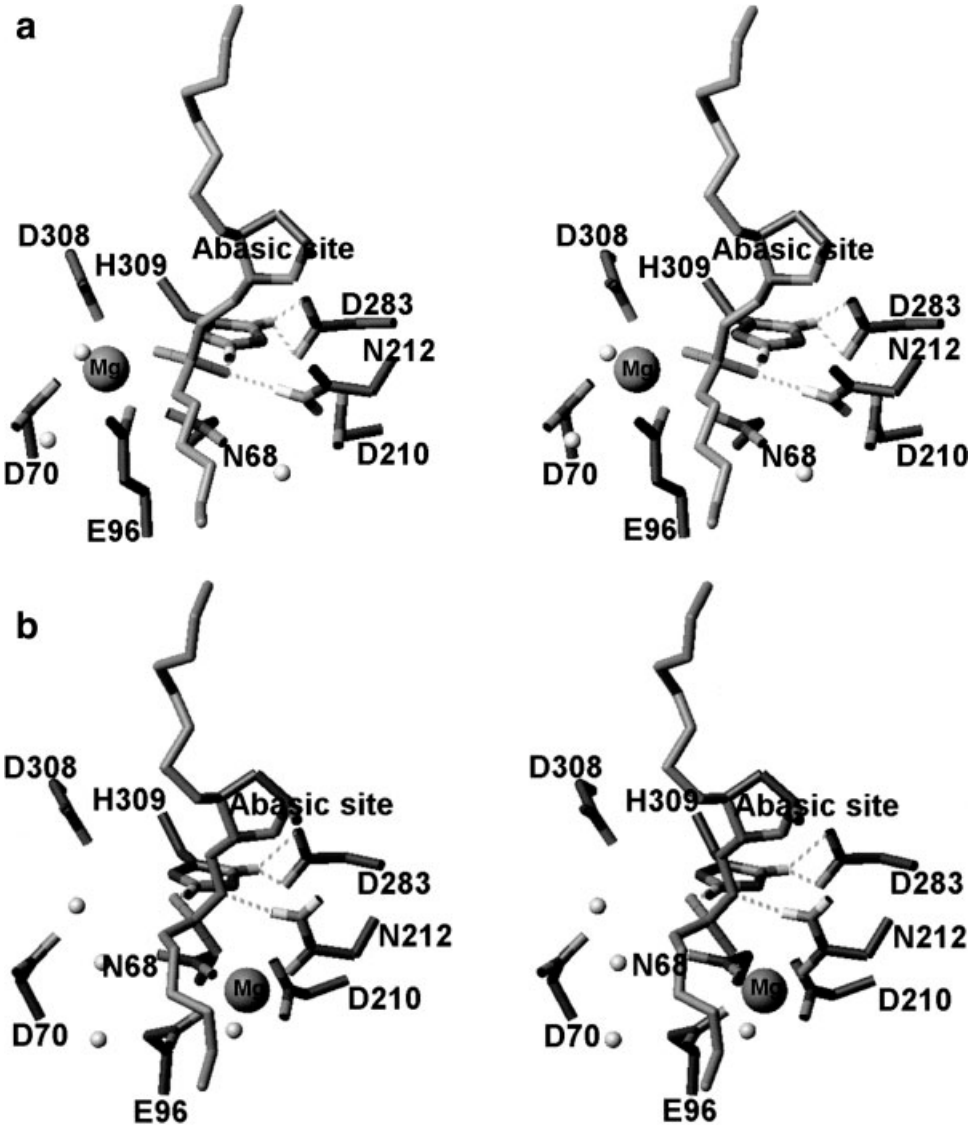

Fig. 2. The figure shows stereo views of the architecture of the A- and B-site important residues at the active site, the DNA back bone, and the abasic site. Hydrogen bonds are shown in dotted lines and water molecules in small spheres. Panel (**a**) shows the active site of the structure with the Mg^{2+} ion at the "grid A-site." Panel (**b**) shows the active site of the structure with the Mg^{2+} ion at the "grid B-site."

3′ end (O3′) of the product moved during the minimization 2.6 Å to a position similar to that seen in the crystal structure with cleaved DNA (1DE9). At the end of the simulations, the Mg^{2+} ion was on the other side of the product and coordinated by N68, D70, E96, D308, and O1P still stabilizing the phosphate (product). The movement of the new 3′ end makes a back reaction impossible. Indeed, this has never been reported in the literature, even though the Mg^{2+} has moved to the right side of the phosphate to be able to catalyze a potential back-reaction.

The metal ion movement depended on the net charges of side chains in the active site. When D210 or H309 were individually protonated, the metal ion did not move further from the minimized position during the simulation. The E96 side chain carboxyl coordinated the metal ion, in both the A-and B-sites, and moved with the metal during simulations as they did in all other simulations. Another essential residue, N212, which stabilized the DNA via H-bonds to the phosphate, O5′, or the sugar oxygens, did not move during the simulations. Whenever the catalytic histidine (H309) was protonated, it formed H-bonds to D283 and one phosphate oxygen and also did not move. This H-bond chain was the closest and thus the most important stabilizing factor for positioning the phosphate and the DNA-backbone bond to be cleaved during the reaction.

Moving Metal Ion Mechanism

Reaction mechanisms for APE1 have been postulated, which involve either one[16] or two ions[18] in preparing the

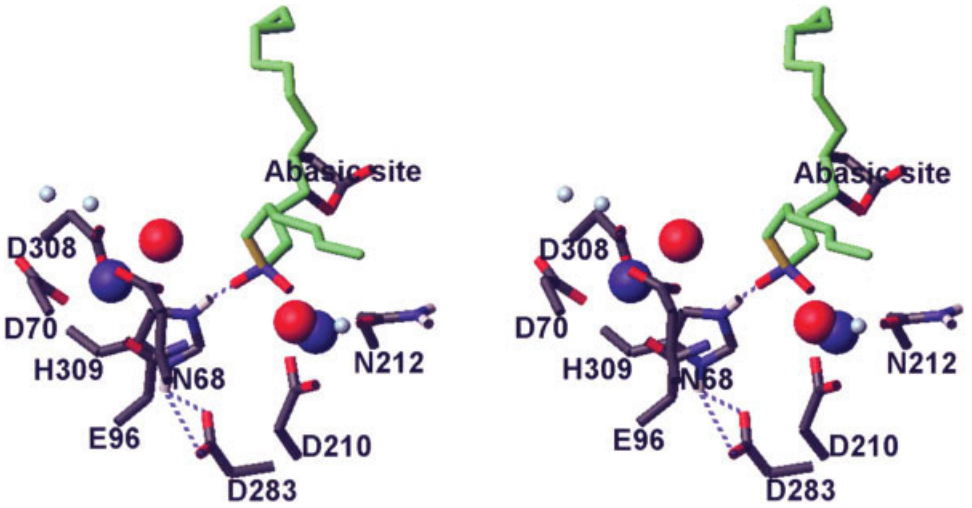

Fig. 3. Stereo view of the active site after 500 ps simulation with uncleaved DNA and protonated H309. Two Mg^{2+} started at the Pb^{2+} positions in 1E9N.The DNA backbone is shown in green and the bond to be cleaved in yellow. Hydrogen bonds are shown in dotted blue and light blue spheres are the water molecules. The distance between the Mg^{2+} ions increased from 5.1 to 7.6 Å during the 500 ps simulation. The final Mg^{2+} positions are shown in blue and the corresponding A- and B-site from the grid search are shown in red.

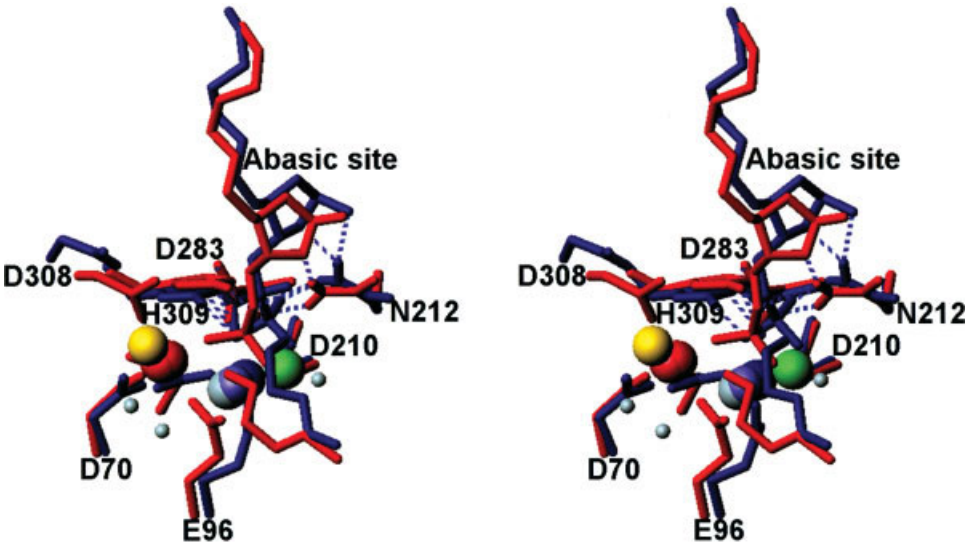

Fig. 4. Stereo views of the active site with cleaved DNA, one Mg^{2+} starting at the B-site, and protonated D210 and H309. Hydrogen bonds are shown in dotted blue. Beginning and end conformations are shown in blue and red. The Mg^{2+} ion started at the B-site (green). The different blue and red shades are positions of the metal before and after its migration from the B- to the A-site. The yellow sphere is the grid A-site with uncleaved substrate.

substrate for cleavage and mediating hydrolysis of a water molecule to generate the attacking OH^-. In the "two-metal" cleavage reaction, one-metal coordinates and stabilizes the leaving group in the transition state, while the other stabilizes the attacking nucleophile (OH^-). However, as shown earlier, the two metal sites of APE1 are not consistent with those in restriction endonucleases and phosphatases that catalyze dimetallic phosphodiester cleavage. Further, the decrease in activity at high Mg^{2+} concentration and the effects of different metals when added simultaneously to the reaction suggest that when both metal sites are occupied, activity decreases[18,49] (Table V).

We thus propose that there is only one-metal ion present during the reaction, which moves between the two sites during and after the reaction to facilitate substrate cleavage. Before cleavage, the metal ion is at the more buried grid B-site and forms a bond with the substrate backbone phosphate oxygen ProR (O2P). It also forms bonds with D210, to facilitate hydrolysis of a water molecule that is also one of its ligands [Figs. 2(b) and 5]. D210 acts as a proton acceptor when the Mg^{2+} bound

TABLE IV. Side Chain Interactions With the Metal Ions (Interatom Distances in Å) in the Active Sites of Two Crystal Structures, Compared With Those in Our Grid Calculations (20 ps), and After the End of 500 ps MD Simulations

	IDE9	1E9N		Grid		MD (A+B)[a]		MD (A+B)[b]		
Atom	A Mn^{2+}	A Pb^{2+}	B Pb^{2+}	Third lowest A Mg^{2+}	Lowest B Mg^{2+}	A Mg^{2+}	B Mg^{2+}	A Mg^{2+}	B Mg^{2+}	MD (B→A)[c]
N68 OD1	4.2	4.9	4.4	5.7	4.0	2.3	6.8	4.4	8.5	1.9
N68 ND2	4.4	4.6	5.7	4.4	5.6	3.6	4.6	4.5	7.2	3.3
D70 OD1	4.1	3.5	8.3	1.9	7.7	1.8	9.2	2.0	9.5	2.0
D70 OD2	5.3	5.1	9.6	3.7	8.4	3.4	11.0	1.9	9.2	2.0
E96 OE1	2.7	2.0	5.9	2.0	1.9	1.9	6.1	1.9	7.1	3.7
E96 OE2	2.6	3.7	7.4	2.0	3.4	2.0	8.1	2.0	6.5	1.9
D210 OD1	7.5	7.8	3.2	8.4	1.9	8.3	1.9	8.3	1.8	6.3
D210 OD2	5.5	6.1	2.8	8.3	2.0	7.4	1.9	8.6	3.5	4.8
N212 OD1	7.2	7.3	3.7	7.7	2.0	9.3	1.9	9.3	1.9	8.7
N212 ND2	9.1	7.3	3.0	7.0	3.8	11.4	4.2	11.0	4.0	6.6
D283 OD1	8.7	10.0	6.5	9.2	7.8	8.9	7.5	9.3	7.2	8.3
D283 OD2	9.1	9.6	6.3	9.2	7.2	8.6	7.3	9.2	6.0	7.6
D308 OD1	3.9	4.6	6.6	3.2	9.0	2.0	8.6	1.9	8.2	3.4
D308 OD2	3.2	4.3	6.8	1.9	7.9	1.9	7.9	1.9	7.5	2.0
H309 NE2	4.2	5.4	3.0	4.7	4.6	5.2	5.5	5.0	4.9	4.3
AP O1P	2.1	—	—	1.9	4.1	5.0	3.7	6.8	1.9	1.9
AP O2P	3.9	—	—	4.2	1.9	6.5	1.8	6.1	1.9	3.9
AP O5′	4.4	—	—	4.3	4.1	7.0	3.7	6.6	2.9	2.5
(AP-1) O3′	2.6	—	—	4.2	3.5	5.2	4.3	3.9	5.4	4.5
Waters O	—	2.8	2.9	2.0	2.0	—	1.9	—	1.9	—

[a]The two Mg^{2+} ions started at the Pb^{2+} positions in 1E9N, the DNA was not cleaved, and H309 was protonated.
[b]Continuation of the simulation, which was started with the two Mg^{2+} ions the 1E9N positions. The DNA was cleaved and H309 and D210 were protonated.
[c]MD simulation with cleaved DNA, protonated D210 and H309. The metal starting position was the B-site. It moved during the simulation to the A-site.

TABLE V. Effect of Ca^{2+} on the APE1 Activity

Ca^{2+} (m*M*)	V_{max} (min^{-1})	K_m (n*M*)
—	13.9 ± 1.6	9.0 ± 7.1
1	7.4 ± 0.8	3.3 ± 2.0
5	2.3 ± 0.2	2.7 ± 0.6

APE1's endonucleolytic cleavage on AP-site containing DNA was analyzed as described previously[36] in a reaction buffer containing 0.5 m*M* $MgCl_2$ and indicated concentrations of $CaCl_2$. Nine different substrate concentrations (0–100 n*M*) were examined for APE1's cleavage activity, and then V_{max}/K_m were obtained by nonlinear regression optimization to the Michaelis–Menten kinetics (experimental data points are given as supplementary material).

water dissociates to generate OH^-, which makes a nucleophilic attack on the DNA back bone at the apurinic site. At this point, the local electrostatics change as the new 3′ end of the cleaved DNA moves away (about 2.6 Å) to the position seen in the crystal structure (1DE9), thereby rendering the reaction irreversible. The new 5′ end, with the phosphate still stabilized by the Mg^{2+} and the H-bonds to H309 and N212, remains stationary in the position of the 1DE9 structure. During the reaction, the metal ion moves immediately about 1.9 Å from the B-site toward the A-site still at the same side of the cleaved DNA. After about 300 ps of simulation, the metal ion migrates 3.3 Å further to the A-site, equivalent to the position seen in the crystal structure 1DE9 [Figs. 4 and 5(b)]. It is now on the other side of the cleaved DNA and octahedrally coordinated by N68, D70, E96, D308, and O1P on the phosphate. Driving forces for movement of the metal into the A-site seen in the 1DE9 crystal structure are the movement of the new 3′ end, the additional proton on the D210 side chain (after accepting the proton to activate the Mg^{2+} bound water), and the inversion of the phosphate group during the reaction, as also previously hypothesized.[16]

DISCUSSION

The major goal of this work was to understand the role of metal ion(s) in facilitating specific cleavage of DNA by APE1. Two different positions for metal ions have been seen in the APE1 active site: the first, the A site, is present in all the crystal structures, while an additional "B" site was suggested by the crystal structure with two Pb^{2+} ions in the active site (1E9N)[18] (Table I). Our grid search (Table II and Fig. 1) indicated that both of the sites are close to local energy minima in the active site of the enzyme (Table III). Thus there are indeed two possible metal ion positions that differ in stability. Further MD simulations showed that the stability of the two sites depended on the protonation state of essential residues in the active site, whether substrate was present, and whether the substrate was cleaved or not (Table IV, Figs. 2 and 3). This data suggested an

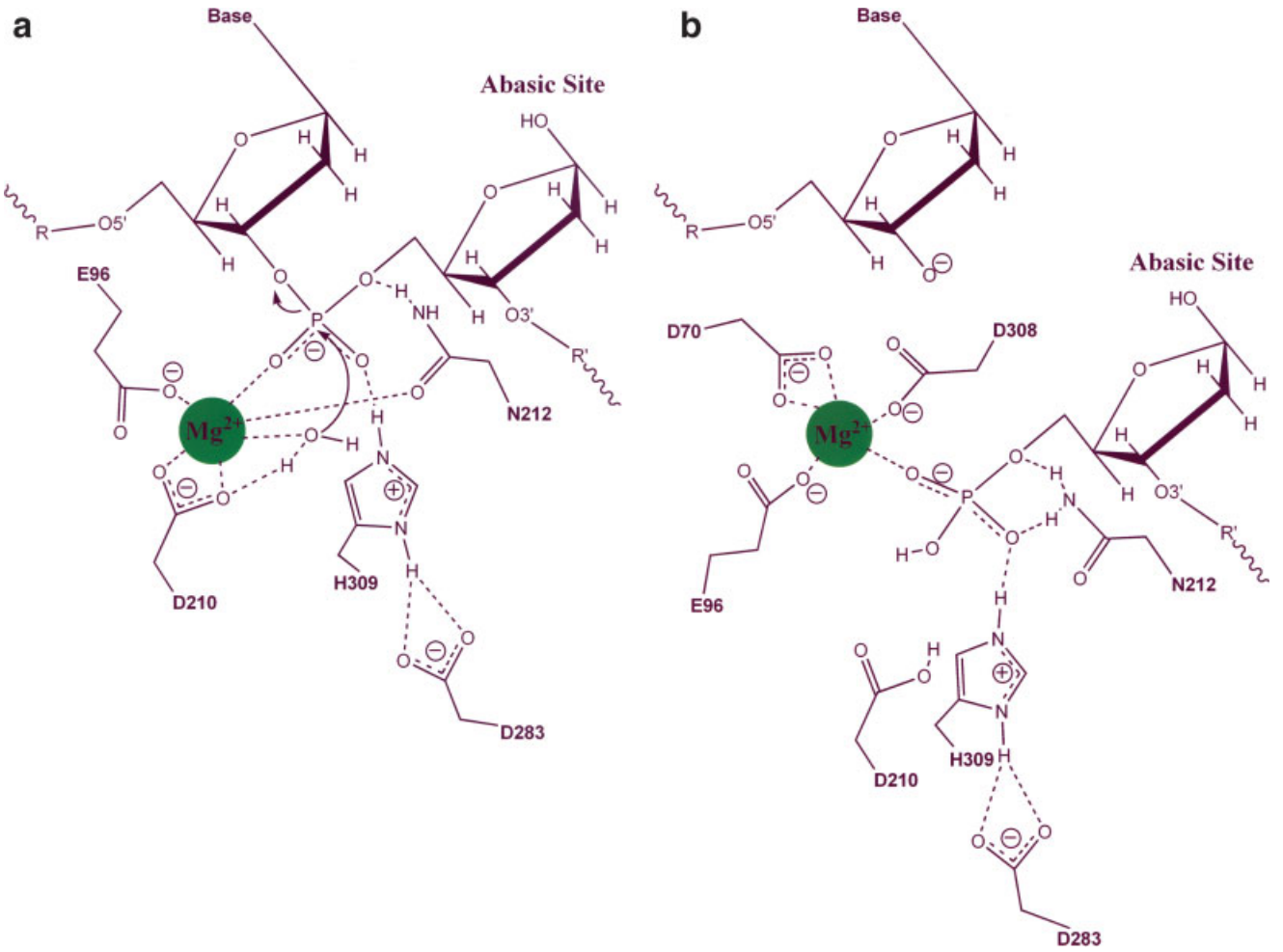

Fig. 5. Schematic drawing of the precleavage (**a**) and after cleavage (**b**) positions of the metal ion and the key ligands in the active site of APE1. For clarity the residues D70 and D308 are not shown in panel (a). At precleavage stage, the phosphate is stabilized by the Mg^{2+} and hydrogen bonds to H309 and N212. A Mg^{2+} bound water is activated, while D210 acts as proton acceptor and the OH^- makes a nucleophilic attack. After cleavage the new 3′ moves away and the Mg^{2+} follows by moving from the ProR position to the other side of the phosphate (ProS).

alternate mechanism for substrate cleavage, in which one-metal ion could move between the two sites during the reaction (see Fig. 4). Later, we show how this mechanism correlates with other experimental data that it is consistent with a more loosely bound metal ion in the active site of APE1, when compared with other enzymes that catalyze metal ion based phosphorolysis[38] and how it contributes to the role of APE1 in the BER pathway.[37,50]

The B-Site is Closer to Residue D210, Which is Essential for Catalysis

One central question remains: if the B-site is stable, why are the catalytically competent metals, such as Mn^{2+}, in the relevant crystal structures closer to the A-site? One could hypothesize that the metals used for the crystal structures are better able to bind at the A-site, which may be favored by the conditions used to obtain the crystallographic complex. Indeed, Mn^{2+} is not an optimal metal for APE1 catalysis (Mg^{2+} gives at least 50× more activity at physiological conditions[49]), and that the pH used for the crystal structure was below the optimum for APE1 activity. Details of the 1DE9 structure suggest that the complex with the metal ion at the A- position is not catalytically competent. The Mn^{2+} ion position in the structure is too far from the side chain oxygens of D210 (>6 Å) to aid in hydrolysis by this residue, and the catalytic H309 is not close enough to the scissile bond to form a H-bond to the phosphate. In contrast, the B-site is within 2 Å of the D210 carboxyl (Table IV), meaning a metal ion would be in position to alter the pKa value of the side chain sufficiently so that it could serve as proton acceptor during hydrolysis of a water.[47] At the same time OH^- would make a nucleophilic attack on the phosphate bond to cleave the DNA backbone. In our mechanism, as the cleavage occurs, the 3′ end of the DNA moves away within the initial minimization and the metal ion swings later into the A-site on the other side of the product (see Fig. 4).

Further evidence for the need for two sites comes from mutagenesis data. In our simulations with one Mg^{2+}, the side chain of E96 always coordinates and moves with the ion, in a sense "bridging" the A- and B-sites. In simulations with two Mg^{2+}, the metal ions are separated by more than 7.7 Å and E96 coordinates only the metal ion at the A-site and is not bridging the two metal sites. Mutation of E96 reduces APE1 activity 600-fold[51] but does not eliminate cleavage entirely. Mutating other residues that form the A-site, N68, D70, and D308,[45,52] also does not eliminate cleavage or substrate binding. On the other hand, mutation of D210 eliminates cleavage but not substrate binding.[53,54] As Table IV illustrates, the carboxyl oxygens of D210 are within 2.0 Å of the B-site. Thus mutational results suggest that both metal sites are required for efficient cleavage, and that precleavage of the metal ion is required to be at the B-site (!), consistent with our proposed mechanism. That is, the metal ion would at this point assist in the disassociation of a water molecule to generate and stabilize the attacking nucleophile, with a carboxyl group of the D210 serving as proton acceptor.

The Two Sites Cannot be Simultaneously Occupied During Catalysis

We previously showed that the architectures of the active site of mono- and dimetallic phosphatases differ.[38] One of the most important aspects of two-metal enzyme active sites, such as the acid phosphatases, is the presence of bridging carboxyl(s) that chelate(s) both metals. These carboxyl(s) mitigate(s) the normal charge repulsion and allows the metals to stay at a relatively close distance to one another, usually between 3 and 4 Å.[47] In all the dimetallic enzymes in that study, the metals are held firmly in place by ionic bonding to several side chains, with short bond distances of <2.0–2.5 Å. In contrast, in APE1 and related enzymes, a single metal is loosely bound, with only the carboxyl of E96 within this distance (Table IV). This relatively unconstrained binding would be consistent with our model for activity, in which the metal must be free to move during the reaction, and to form bonds with the substrate before and after cleavage.

The distance between the "grid-A" and "grid-B" positions is 5.7 Å, similar to intermetal distances in restriction edonucleases. However, when two Mg^{2+} ions are placed in the active site their distance increases to 7.7 Å.

Other data indicate that both metal sites cannot be occupied during cleavage. Kinetic studies of APE1 in the presence of different metal ions showed that enzymatic activity was reduced at high metal ion concentration, where both sites could be expected to be filled.[18,45,49,55] Further, at low Mg^{2+} concentration (0.5 mM) additional amount of Ca^{2+} reduced the activity (Table V). However this data is in contradiction to a similar experiment by Beernink et al.[18] where the total ion concentration (Mg^{2+} + Ca^{2+}) was kept constant at 10 mM and additional Ca^{2+} (>7 mM) slightly enhanced the relative activity at Mg^{2+} concentrations <3 mM. This kind of enhancement of the activity by Ca^{2+} was reported for EcoRV[56] when Mn^{2+} was used instead of Mg^{2+}. Negative effect on the activity by Ca^{2+} was reported[56] for Mg^{2+} as we see it for APE1 (Table V).

Our data accounts for why simultaneous occupancy of the two sites would not support catalysis. Thus it is reasonable to assume that only one Mg^{2+} ion is present in the active site of APE1 as we see it in the crystal structure (1DE9) with the product bound to the protein.[16]

Moving Metal Mechanism Enables the Enzyme to Irreversibly Cleave Its Substrate While Still Retaining the Product for Passage to Other Enzymes in the BER Pathway

Phosphatase reactions are typically terminated by an assumed free diffusion of the product. However, as we noted previously,[37] the last part of APE1's activity in the BER pathway is to retain the product of the reaction until it can be passed to the next enzyme in the pathway.[57] The enzyme's active site is thus more processive than its sister enzyme, DNase 1. Conserved residues that differ between APE1 and DNase 1 mediate bonds to the opposite (uncleaved) strand of the DNA from the damaged (cleaved) strand, enabling APE1 to bind firmly to its product, and facilitate the binding of the next enzyme in the BER pathway to the properly oriented DNA. This means that the enzyme must terminate the reaction, but retain the product until it can be properly transferred.

In our mechanism, the metal ion assists in this effort, by moving from a catalytically active position to one in which it facilitates retention of the cleaved product (Figs. 4 and 5). The new 3′ end of the product moves 2.6 Å making the reaction irreversible while the phosphate remains tightly bound to the Mg^{2+} and via hydrogen bonds to H309 and N212. For example, one mutant, H309N, abolishes activity and increases substrate release by 10 fold.[46,53] According to NMR results, H309 forms a very strong hydrogen bond to D283[58] and our simulations show a second hydrogen bond to the phosphate of the substrate/product. The mutation, D283A, disturbs the H-bond network and enhances product release.[45] None of the hydrogen bonds to these residues are disturbed during our *in silico* cleavage reaction.

In conclusion, our MD results, coupled with analysis of mutagenesis data, suggested that while only one-metal ion is sufficient for nucleophilic catalysis, this metal ion needs to move between two binding sites on the protein and the DNA during the reaction. This dynamic view of catalysis can explain much of the experimental data.

ACKNOWLEDGMENTS

We thank Roman Osman at Mount Sinai School of Medicine, Physiology and Biophysics Department, New York, for providing the force field parameter for the uncleaved AP site. Computational support was provided

by the National Computational Science Alliance (NCSA) (SGI/CRAY Origin2000) and was used to develop the force field parameters for the cleaved AP site.

REFERENCES

1. Lindahl T, Nyberg B. Rate of depurination of native deoxyribonucleic acid. Biochemistry 1972;11:3610–3618.
2. Holmquist GP. Endogenous lesions, S-phase-independent spontaneous mutations, and evolutionary strategies for base excision repair. Mutat Res 1998;400:59–68.
3. Dianov GL, Sleeth KM, Dianova II, Allinson SL. Repair of abasic sites in DNA. Mutat Res 2003;531:157–163.
4. Zharkov DO, Grollman AP. Combining structural and bioinformatics methods for the analysis of functionally important residues in DNA glycosylases. Free Radic Biol Med 2002;32:1254–1263.
5. Osman R, Fuxreiter M, Luo N. Specificity of damage recognition and catalysis of DNA repair. Comput Chem 2000;24:331–339.
6. Strauss PR, O'Regan ME. Abasic site repair in higher eukaryotes. In: Nickoloff JA, Hoekstra MF, editors. DNA damage and repair, Vol. 3. Totowa, NJ: Humana; 2001. pp 43–85.
7. Hickson ID, Gorman MA, Freemont PS. Structure and functions of the major human AP endonuclease HAP1/Ref-1. In: Nickoloff JA, Hoekstra MF, editors. DNA damage and repair, Vol. 3. Totowa, NJ: Humana; 2001. pp 87–105.
8. Evans AR, Limp-Foster M, Kelley MR. Going APE over ref-1. Mutat Res 2000;461:83–108.
9. Lindahl T. Suppression of spontaneous mutagenesis in human cells by DNA base excision-repair. Mutat Res 2000;462:129–135.
10. Wilson SH. Mammalian base excision repair and DNA polymerase β. Mutat Res 1998;407:203–215.
11. Wilson DMI, Barsky D. The major human abasic endonuclease: formation, consequences and repair of abasic lesions in DNA. Mutat Res 2001;485:283–307.
12. Mol CD, Hosfield DJ, Tainer JA. Abasic site recognition by two apurinic/apyrimidinic endonuclease families in DNA base excision repair: the 3′ ends justify the means. Mutat Res 2000;46:211–229.
13. Demple B, Harrison L. Repair of oxidative damage to DNA—enzymology and biology. Annu Rev Biochem 1994;63:915–948.
14. Bennett RA, Wilson DM, III, Wong D, Demple B. Interaction of human apurinic endonuclease and DNA polymerase β in the base excision repair pathway. Proc Natl Acad Sci USA 1997;94:7166–7169.
15. Vidal AE, Boiteux S, Hickson AD, Radicella JP. XRCC1 coordinates the initial and late stages of DNA abasic site repair through protein–protein interactions. EMBO J 2001;20:6530–6539.
16. Mol CD, Izumi T, Mitra S, Tainer JA. DNA-bound structures and mutants reveal abasic DNA binding by APE1 and DNA repair coordination. Nature 2000;43:451–456.
17. Gorman MA, Morera S, Rothwell DG, de La Fortelle E, Mol CD, Tainer JA, Hickson ID, Freemont PS. The crystal structure of the human DNA repair endonuclease HAP1 suggests the recognition of extra-helical deoxyribose at DNA abasic sites. EMBO J 1997;16:6548–6558.
18. Beernink PT, Segelke BW, Hadi MZ, Erzberger JP, Wilson DM, III, Rupp B. Two divalent metal ions in the active site of a new crystal form of human apurinic/apyrimidinic endonuclease, Ape1: implications for the catalytic mechanism. J Mol Biol 2001;307:1023–1034.
19. Chevalier BS, Monnat RJ, Jr, Stoddard BL. The homing endonuclease I-CreI uses three metals, one of which is shared between the two active sites [see comment]. Nat Struct Biol 2001;8:312–316; erratum 473.
20. Conlan LH, Dupureur CM. Dissecting the metal ion dependence of DNA binding by PvuII endonuclease. Biochemistry 2002;41:1335–1342.
21. Etzkorn C, Horton NC. Mechanistic insights from the structures of hincll bound to cognate DNA cleaved from addition of Mg^{2+} and Mn^{2+}. J Mol Biol 2004;343:833–849.
22. Horton NC, Perona JJ. Making the most of metal ions. Nat Struct Biol 2001;8:290–293.
23. Etzkorn C, Horton NC. Ca^{+} binding in the active site of HincII: implications for the catalytic mechanism. Biochemistry 2004;43:13256–13270.
24. Jose TJ, Conlan LH, Dupureur CM. Quantitative evaluation of metal ion binding to PvuII restriction endonuclease. J Biol Inorg Chem 1999;4:814–823.
25. Pingoud A, Jeltsch A. Recognition and cleavage of DNA by type-II restriction endonucleases. Eur J Biochem 1997;246:1–22.
26. Kostrewa D, Winkler FK. Mg^{2+} Binding to the active-site of EcoRV endonuclease—a crystallographic study of complexes with substrate and product DNA at 2-Å resolution. Biochemistry 1995;34:683–696.
27. Thomas MP, Brady RL, Halford SE, Sessions RB, Baldwin GS. Structural analysis of a mutational hot-spot in the EcoRV restriction endonuclease: a catalytic role for a main chain carbonyl group. Nucleic Acids Res 1999;27:3438–3445.
28. Horton NC, Perona JJ. DNA cleavage by EcoRV endonuclease: two metal ions in three metal ion binding sites. Biochemistry 2004;43:6841–6857.
29. Horton NC, Newberry KJ, Perona JJ. Metal ion-mediated substrate-assisted catalysis in type II restriction endonucleases. Proc Natl Acad Sci USA 1998;95:13489–13494.
30. Truong NT, Naseri JI, Vogel A, Rompel A, Krebs B. Structure–function relationships of purple acid phosphatase from red kidney beans based on heterologously expressed mutants. Arch Biochem Biophys 2005;440:38–45.
31. Bauer-Siebenlist B, Meyer F, Farkas E, Vidovic D, Dechert S. Effect of Zn center dot center dot center dot Zn separation on the hydrolytic activity of model dizinc phosphodiesterases. Chem Eur J 2005;11:4349–4360.
32. O'Brien PJ, Herschlag D. Does the active site arginine change the nature of the transition state for alkaline phosphatase-catalyzed phosphoryl transfer? J Am Chem Soc 1999;121:11022–11023.
33. Hwang KY, Baek K, Kim HY, Cho Y. The crystal structure of flap endonuclease-1 from *Methanococcus jannaschii*. Nat Struct Biol 1998;5:707–713.
34. Zhang J, Zhang ZJ, Brew K, Lee EYC. Mutational analysis of the catalytic subunit of muscle protein phosphatase-1. Biochemistry 1996;35:6276–6282.
35. Lai KH, Dave KI, Wild JR. Bimetallic binding motifs in organophosphorus hydrolase are important for catalysis and structural organization. J Biol Chem 1994;269:16579–16584.
36. Izumi T, Schein CH, Oezguen N, Feng YL, Braun W. Effects of backbone contacts 3′ to the abasic site on the cleavage and the product binding by human apurinic/apyrimidinic endonuclease (APE1). Biochemistry 2004;43:684–689.
37. Schein CH, Ozgun N, Izumi T, Braun W. Total sequence decomposition distinguishes functional modules, "molegos" in apurinic/apyrimidinic endonucleases. BMC Bioinformatics 2002;3:37.
38. Schein CH, Zhou B, Oezguen N, Mathura VS, Braun W. Molego-based definition of the architecture and specificity of metal-binding sites. Proteins-Struct Funct Bioinformatics 2005;58:200–210.
39. Jorgensen WL, Chandrasekhar J, Madura JD. Comparison of simple potential functions for simulating liquid water. J Chem Phys 1983;79:926–935.
40. Besler BH, Merz KMJ, Kollman PA. Atomic charges derived from semiemperical methods. J Comput Chem 1990;11:431–439.
41. Singh UC, Kollman PA. An approach to computing electrostatic charges for molecules. J Comput Chem 1984;5:129–145.
42. Frisch MJ, Trucks GW, Schlegel HB, Scuseria GE, Robb MA, Cheeseman JR, Zakrzewski VG, Montgomery JA, Jr, Stratmann RE, Burant JC, Dapprich S, Millam JM, Daniels AD, Kudin KN, Strain MC, Farkas O, Tomasi J, Barone V, Cossi M, Cammi R, Mennucci B, Pomelli C, Adamo C, Clifford S, Ochterski J, Petersson GA, Ayala PY, Cui Q, Morokuma K, Salvador P, Dannenberg JJ, Malick DK, Rabuck AD, Raghavachari K, Foresman JB, Cioslowski J, Ortiz JV, Baboul AG, Stefanov BB, Liu G, Liashenko A, Piskorz P, Komaromi I, Gomperts R, Martin RL, Fox DJ, Keith T, Al-Laham MA, Peng CY, Nanayakkara A, Challacombe M, Gill PMW, Johnson B, Chen W, Wong MW, Andres JL, Gonzalez C, Head-Gordon M, Replogle ES, Pople JA. Gaussian 98. Pittsburgh, PA: Gaussian, Inc.; 2001.
43. Wang J, Cieplak P, Kollman PA. How well does a restrained electrostatic potential (RESP) model perform in calculating conformational energies of organic and biological molecules. J Comput Chem 2000;21:1049–1074.

44. Koradi R, Billeter M, Wuthrich K. MOLMOL: a program for display and analysis of macromolecular structures. J Mol Graph 1996;14:51–55.
45. Masuda Y, Bennett RAO, Demple B. Rapid dissociation of human apurinic endonuclease (Ape1) from incised DNA induced by magnesium. J Biol Chem 1998;273:30360–30365.
46. Masuda Y, Bennett RAO, Demple B. Dynamics of the interaction of human apurinic endonuclease (Ape1) with its substrate and product. J Biol Chem 1998;273:30352–30359.
47. Glusker JP, Katz AK, Bock CW. Two-metal binding motifs in protein crystal structures. Struct Chem 2001;12:323–341.
48. Beese LS, Steitz TA. Structural basis for the 3′-5′ exonuclease activity of *Escherichia coli* DNA polymerase I: a two metal ion mechanism. EMBO J 1991;10:25–33.
49. Barzilay G, Mol CD, Robson CN, Walker LJ, Cunningham RP, Tainer JA, Hickson ID. Identification of critical active-site residues in the multifunctional human DNA repair enzyme HAP1. Nat Struct Biol 1995;2:561–568.
50. Zhu H, Braun W. Sequence specificity, statistical potentials, and three-dimensional structure prediction with self-correcting distance geometry calculations of β-sheet formation in proteins. Protein Sci 1999;8:326–342.
51. Izumi T, Malecki J, Chaudhry MA, Weinfeld M, Hill JH, Lee JC, Mitra S. Intragenic suppression of an active site mutation in the human apurinic/apyrimidinic endonuclease. J Mol Biol 1999; 287:47–57.
52. Erzberger JP, Wilson DM, III. The role of Mg^{++} and specific amino acid residues in the catalytic reaction of the major human abasic endonuclease: new insights from EDTA-resistant incision of acyclic abasic site analogs and site-directed mutagenesis. J Mol Biol 1999;290:447–457.
53. Rothwell DG, Hang B, Gorman MA, Freemont PS, Singer B, Hickson ID. Substitution of Asp-210 in HAP1 (APE/Ref-1) eliminates endonuclease activity but stabilises substrate binding. Nucleic Acids Res 2000;28:2207–2213.
54. Nguyen LH, Barsky D, Erzberger JP, Wilson DMI. Mapping the protein–DNA interface and the metal-binding site of the major human apurinic/apyrimidinic endonuclease. J Mol Biol 2000;298:447–459.
55. Chattopadhyay R, Wiederhold L, Szczesny B, Boldogh I, Hazra TK, Izumi T, Mitra S. Identification and characterization of mitochondrial abasic (AP)-endonuclease in mammalian cells. Nucleic Acids Res 2006;34:2067–2076.
56. Vipond IB, Baldwin GS, Halford SE. Divalent metal ions at the active sites of the EcoRV and EcoRI restriction endonucleases. Biochemistry 1995;34:697–704.
57. Lloyd RS. Processicity of DNA repair enzymes. In: Schein CH, editor. Nuclease methods and protocols, Vol. 160. Totowa, NJ: Humana; 2001. pp 3–14.
58. Lucas JA, Masuda Y, Bennett RA, Strauss NS, Strauss PR. Single-turnover analysis of mutant human apurinic/apyrimidinic endonuclease. Biochemistry 1999;38:4958–4964.